

LANFORD 1994

Land Management Program

THE CAUCA PROJECT

1994-1995

Mitch Lanfort



THE CAUCA PROJECT (Land Management Program)

The study area for this project is located in the Cauca Department, which of Colombia. It lies approximately 50km south of the city of Cali, and is centered on the geographic coordinates ($76^{\circ} 30'W$, $2^{\circ} 40'N$). The total area of interest extends to approximately ?? km², and within this region altitudes range from ?? m to ?? m above sea level.

Climate: Mean Annual Temp/Rainfall/Seasons

Vegetation: Natural vegetation would be....

Now replaced by...

{note spatial scale and complexity of land cover/use}

The local economy is based on agriculture (subsistence + cash crops)

Occupation of hill tops, with lines of communication running along crests

Farming extending down the slopes towards the valley bottoms.

Although the topography is complex when viewed in detail, it has the general structure of a deeply dissected but gently sloping (which direction, S->N?) plateau. Slope gradients are typically high(?) and fall within the range of 0° up to ??°. Slope orientations vary widely and overall are approximately isotropic. Drainage is achieved via a number of rivers flowing approximately parallel from SE to NW. These are all tributaries of the Ovejas River which discharges into the Cauca River on the western limits of the study area. The study area is largely defined by the Ovejas watershed. However, within this watershed the tributaries to the Ovejas define a number of micro-watersheds, and amongst these the Rio Cabuyal has been selected for detailed study. Covering an area of ?? hectares, this micro-watershed is believed to be representative of the topography, agriculture and natural vegetation of the whole entire region.

Aims:

The first aim in this project is simply to derive land cover information for the study area.

Information about basic land cover has been absent to date, but it is essential for a wide range of modelling procedures. These are concerned with: hydrology and water balance (e.g. Topog_IRM), the study of nutrient movements, a better understanding of soil development, and assessment of sediment movements and erosion. The ultimate aim of this modelling will be to assist in the identification and development of sound agricultural practices. These can be defined as those systems that provide high productivity that is sustainable and which does not cause environmental degradation.

A map of current land cover will also act as a bench mark against which future land cover changes can be assessed, and will allow strategic planning to be undertaken. Although not an immediate concern, it is hoped that archival data in the form of Landsat MSS imagery and air photography will eventually allow historical land cover changes to be assessed, perhaps as far back as 1940. There are, however, many technical difficulties to be overcome if this objective is eventually to be met. As an example, there will be a problem in matching the thematic information obtainable from the Landsat TM and SPOT HRV scanners used in the present study, to that which can be derived from the MSS scanner with its lower spatial and spectral resolution.

1.10.1985

The same problem of equating information between sensors of differing capabilities also arises in respect to another future aim of the GIS Land Management Group. Namely that, once it is established for the Cabuyal and Ovejas catchments, the group will be interested in extending land cover mapping to larger scales within Colombia and to other regions of the Tropics. On both logistical (ie data volume) and cost grounds it is certain that relatively coarse resolution imagery such as that provided by the MSS will need to be utilised. The accuracy and usability of MSS derived products need to be quantified and assessed in respect to higher resolution counterparts. Again, there are many potential difficulties and problems which lie ahead when attempting to equate information across sensors and scales (see, for example, Moody and Woodcock, 1994). However, a methodology in which MSS data is used to provide a general inventory, with TM/HRV and air photographs employed for detailed study in specific environments, is very appealing.

Objectives:

At a meeting held with the Hillside Group, a hierarchical land cover classification scheme was developed. Each level in this scheme would provide data of value and interest to the group. As thematic discrimination increases within these levels, the technical difficulties in achieving the product become more complex. The basic plan was to 'start at the easy end' and work towards the more ambitious products.

(I)	(II)	(III)
LOW...	erosion... fallow...	"infrastructure" "natural processes" fallow
	arable...	other casava modern coffee traditional coffee
MEDIUM...	pasture...	good quality poor quality
HIGH...	woodland...	primary forestry poor quality secondary good quality secondary managed reforestation bamboo

The main objectives were quite simply;

- (1) Derive a classification at Level (I)
- (2) Derive a classification at Level (II)
- (3) Derive a classification at Level (III)

{definition of detailed study area}

{details of data and imagery available}

{details of hardware/software}

{details of pre-processing to establish the basic database}

Image Enhancement and Information Extraction

There are a great many possibilities for enhancing the visual appearance of the images, and for transforming the radiometric data into more meaningful information.

These include:

Contrast Enhancements
Decorrelation Stretch

Spatial Enhancement (e.g. spatial domain filtering)
Spectral Merges (SPOT Pan./Landsat TM/SPOT XS)

Band Ratios
DEM based topographic corrections

Principal Components Analysis
Other empirical transformations (e.g. Tasseled Cap)

Computation of spatial properties (edge density, texture etc)

Classification

where a number of alternatives arise...

- Unsupervised vs Supervised

-use of spectral bands only?

-include spatial information?

-include DEM information?

- hard classification?

- soft classification

maximum likelihood vectors

2nd most likely classes

spectral unmixing

fuzzy classes

- use post-classification filtering?

- use post-classification knowledge-based adjustments?

- use post-classification constraint-based adjustments?

- method of classification accuracy assessment

The principal purpose of all these procedures are to:

- Improve the visual display and aid manual image interpretation.
- Reduce uneven scene illumination due to topographic orientation, and negate its impact on the spectral signatures of land covers.
- Suppress common information between bands, and enhance spectral differences.
- Exploratory data analysis and dimensionality reduction
- Transformation of radiometric data to environmental information e.g. LAI, soil wetness, vegetation stress, etc.
- Transform radiometric vectors into nominal information classes or probabilistic functions.

Such a wide range of possibilities creates a certain dilemma when planning a project. Which of the many possible avenues of image enhancement, transformations, classification schemes, additional datasets, etc should be followed.

In this particular instance there were two over-riding factors which shaped the direction of the work undertaken:

(a) the complex topographic environment, with steep slopes of all orientations

(b) the highly complex land use patterns, which are in themselves largely a result of the complex topographic environment. Individual farms are typically only ?? Ha in extent, and land use or land cover can change over a distance of ?? m. However, the diversity of arable crops is quite remarkable, although there is a certain degree of transience in the exact composition, driven by the market forces of cash cropping.

A key problem to be dealt with in this region is the potentially adverse influence of the complex topography on spectral signatures. Any attempt at a classification of land cover is likely to be influenced by topographic orientation in addition to the spectral signatures generated by differing land cover classes.

Topographic effects within the major valleys are clearly visible in the images derived from all three sensors. Furthermore, although they may not be so immediately apparent to the eye, it must be assumed that spectral signatures are equally influenced on a local pixel-by-pixel scale by the rapid changes in slope gradient and aspect over relatively short distances.

As a quick test of this assumption an unsupervised classification (ISODATA) was performed on the TM imagery and the correspondance of the spectral clusters with the slope and aspect maps derived from the DEM. Even by eye, it was immediately apparent that topography in isolation was having a significant influence on spectral responses.

{{chi-square of aspect/spectral class - being close to equator approx even number of days of sun N/S, and even hours E/W, so no reason to suppose topography should have a strong influence on vegetation composition} use matrix, then take a random sample, then build matrix and put into

minitab}

One solution to this problem is to treat the spectral signatures that are generated by a given land cover occurring on the 'dark' and 'light' sides of a valley as separate signatures during the classification process, and then to collapse this distinction in a post-classification stage.

This is rather crude since the distribution of slope aspects in the region is by no means bimodal, and thus a two-fold division of dark-light will incorporate considerable within-class-variability.

Band Ratios

The 'classic' approach to solving this problem is to compute the ratio values between spectral bands. There are a number of reported examples where ratios have been found to be an effective solution (e.g. Hoben and Justice (1981), **).

However, excluding the thermal band there are 15 possible ratio combinations within the TM imagery. Thus, already, while potentially solving one problem this method can create another, namely which ratios to use?

1	1:2	2	1:3	3	1:4
4	1:5	5	1:7	6*	2:3
7	2:4	8	2:5	9	2:7
10*	3:4	11*	3:5	12	3:7
13*	4:5	14*	4:7	15*	5:7

So some extent arbitrarily, but with some respect of the current literature and an understanding of spectral signatures, the ratios indicated by * were computed.

Initial visual interpretation of the ratio data sets.

(4:3, 5:3) moderate topographic suppression
4:3 shows vegetation quantity
5:3 shows the clearest bare soil differentiation,
but very little separation between vegetation types

(5:4, 7:4, 7:5) very good topographic suppression
5:4 looks as if it provides good vegetation discrimination
7:4 similar in appearance to 5:4
7:5 same again, but a higher noise component

(3:2) moderate to poor topographic suppression
3:2 is generally noisy, unsure of information content

Many of the derived ratio images were, as might be expected, visually similar. To gain some measure of the degree of similarity a correlation matrix was computed between the ratios identified above and is presented in Table 1. This illustrates that the correlation relationships fall broadly into three categories:

(i) Very high
(5:4) & (7:4) 0.96

(4:3) & (3:2) 0.81
 (7:5) & (7:4) 0.89

(ii) High
 ...the rest...

(ii) Low
 (5:4) & (5:3) 0.10
 (7:4) & (5:3) 0.19
 (7:5) & (5:3) 0.31
 (3:2) & (5:3) 0.39

Table 1: Correlation Table for Band Ratio Images

Ratio	5:4	5:3	4:3	7:5	7:4	3:2
5:4	1.0000	-0.1016	-0.7895	0.7769	0.9600	0.7749
5:3		1.0000	0.6175	-0.3157	-0.1930	-0.3971
4:3			1.0000	-0.7601	-0.7843	-0.8116
7:5				1.0000	0.8904	0.7409
7:4					1.0000	0.7743
3:2						1.0000

{spectral distances and band combinations}

PCA Transformation

PCA is a linear combination that provides a rotation of the measurement axes in the feature space such that whilst remaining orthogonal they are aligned along the directions of greatest variance. Due to its derivation from the covariance/correlation between spectral bands the properties of a PCA is scene-dependant. It has been used for dimensional reduction and data compression as well as for the exploratory analysis of data structure. Higher components can often reveal subtle information not seen in the original spectral bands. There are numerous examples of its use in RS applications (eg ** **). It was applied in this case for several reasons..

- (1) To help understand the information content within the TM image
- (2) To investigate the potential of using the PCA components in place of the original spectral bands
- (3) To assess its ability to reduce dimensionality - which may become important if additional information layers were to be used in a maximum likelihood classification.

The correlation table for the TM bands (Table 2) shows the high interband correlations typical for imagery derived from this sensor. Particularly highly correlations occur between the visible bands, and also between Band 5 & Band 7.

Table 2: Correlation Table for the Landsat TM imagery

Band	1	2	3	4	5	7
1	1.0000	0.9515	0.9197	0.2907	0.6202	0.6978
2		1.0000	0.9568	0.3780	0.7073	0.7568
3			1.0000	0.2438	0.7505	0.8354
4				1.0000	0.4670	0.2287
5					1.0000	0.9265
7						1.0000

The eigenvalues, when re-expressed as a cumulative percentage, demonstrate the potential value of a PCA transformation on this data set in reducing dimensionality with minimal loss of information. As shown in Table 3, the first three PCA bands carry over 98% of the total scene variance.

Table 3: Eigenvalues from PCA transformation of TM data

Component	Eigenvalue	%variance	%cumulative
I	651.73	70.87	70.87
II	168.64	18.34	89.22
III	87.28	9.49	98.71
IV	5.90	0.64	99.35
V	4.64	0.50	99.86
VI	1.32	0.14	100.00

Table 4: Component Loadings

	I	II	III	IV
1	0.3403	-0.2084	-0.6360	0.5968
2	0.2321	-0.0919	-0.3294	-0.1926
3	0.3255	-0.2386	-0.3294	-0.6049
4	0.3020	0.9134	-0.1968	-0.1278
5	0.7045	-0.0251	0.5476	0.3011
6	0.3696	-0.2369	0.1998	-0.3658

The component loadings are shown in Table 4. These show that PCA-1 is an approximately evenly weighted average of all spectral bands. PCA-2 is dominated by the information carried in TM Band 4, and PCA-3 picks up most information from TM Bands 1 & 5.

In an initial visual interpretation of PCA images the following comments were made:

PCA-1 Overall luminance across the sampled spectrum, or "brightness"
Topographic detail and shadowing is very clear

PCA-2 Vegetation "lushness". This appears to match closely both the
Tasseled Cap "greenness" and the 4:3 ratio (check via correls)

PCA-3 Separates valley bottoms and hill tops. Both vegetation and topo info present
Appears to be an inverse of the Tasseled Cap "wetness"
Thus it could be termed "dryness"?

PCA-4+ Were dominated by scanner and background noise
and thus disregarded. They account for < 2% of total variance.

Since the topographic effect appears to be concentrated in PCA-1, one possibility is to "discard" this band and to use the remaining PCA bands in a classification scheme, thereby removing the topographic effect. However, with the loss of 70% of total scene variance, it is unlikely that this would provide a good solution. Nevertheless, the fact that hyperspectral "intensity" is concentrated in PCA-1 is beneficial. It allows the possibility of "correcting" this information in isolation from the other thematic information.

Tasseled Cap Transformation

This procedure is based on a similar translation of the measurement axes in feature space. It is designed for vegetation studies, and the measurement axes have been rotated in such a fashion as to record information relating to dominant environmental influences: (Axis 1 = soil brightness, Axis 2 = vegetation biomass, Axis 3 = soil and canopy moisture).

Unlike PCA, the rotation of the axes are not determined by scene variance but are a fixed translation determined by empirical observation. Originally defined for MSS data, then extended to TM (refs to Crist). For TM data Christ et al. defined four principal information carriers, termed "brightness", "greenness", "wetness", and "haze". One potentially big advantage of the tasseled cap is for cross-scene comparisons, but the degree to which the interpretations described above match a particular scene under study is somewhat arguable. Since a Tasseled Cap is defined for MSS data also, it may be useful to compare the results of a TM and MSS based Tasseled Cap transformation for the same study region (a future project perhaps). If these prove compatible it would provide a 'link' between TM and MSS data to allow transitions across scale.

The Tasseled Cap and PCA transformations displayed very similar information. The visual similarity is borne out by the correlation matrix shown in Table 5. Clearly, the Tasseled Cap and PCA are to a large degree measuring the same information.

TS1 & PCA 1 (0.98)
TS2 & PCA 2 (0.95)
TS3 & PCA 3 (0.64)

This implies that the Tasseled Cap transformation is effectively capturing the dominant information content of the 6 TM bands. A distinct advantage of the Tasseled Cap over the PCA transformation is that the consistency of the axes rotation allows cross-scene comparisons, something not possible

with PCA.

Table 5: Correlation Table for PCA (Ratio 4:3) and the Tasseled Cap

Band	PC1	PC2	PC3	TC1	TC2	TC3
PC1	1.0000	0.0000	0.0000	0.9818	-0.2337	-0.6783
PC2		1.0000	0.0000	0.1506	0.9459	0.3553
PC3			1.0000	-0.1081	0.2192	-0.6384
TC1				1.0000	-0.1118	-0.5424
TC2					1.0000	0.3516
TC3						1.0000

However, in both the Tasseled Cap and the PCA images a noticeable residual topographic effect is present in the non-"brightness" bands. The band ratio images appeared to be more successful in this respect.

Backwards Radiance Correction and Spectral Merging

The literature suggests that spectral merging of SPOT PAN and TM is profitable (e.g. Carper *et. al.*, 1990; Chavez *et. al.*, 1991; Cliche G *et. al.*, 1985; Harris *et. al.*, 1990; Shettigara, 1992; Welch and Ehlers, 1987). This can be achieved by an RGB-to-IHS transform, replacing the intensity layer with the panchromatic data, and then reversing the process using IHS-to-RGB. Alternatively, it is possible to perform a PCA transformation, relace the Component-I image with the high resolution (panchromatic) band and then apply the inverse PCA transformation. (note: best to use PCs based on correlation matrix, not the covariance matrix).

The aim of this process is to combine the thematic "richness" of the TM imagery with the spatial detail of the SPOT HRV panchromatic data. Clearly, this is a tempting choice in this application where land cover is so spatially variable. Higher spatial resolution is a distinct advantage in providing an accurate land cover map. However, to use this procedure would still leave the topographic effect to be dealt with. Taking ratios between bands after performing a spectral merge is becoming rather "messy" and convoluted. Furthermore, the effect of the ratio operation will be to largely suppress the information that has just been supplied by incorporating the SPOT panchromatic band anyway (#i think#).

The literature also suggests that topographic correction is more effective if based on a backwards radiance correction transformation (BRCT) rather than relying on band ratios (Civco, 1989; Conese *et. al.*, 1993; Colby, 1991; Justic *et. al.*, 1981; Naugle and Lashlee, 1992). This, of course, has greater demands in the sense that it requires a suitable DEM for the region (i.e. at an appropriate accuracy and scale). However, the use of additional information should enable

Thus, to negate the effects of topographic orientation and achieve as high a level of spatial detail as possible it was decided to attempt to combine these two procedures.

ie:

- 1) Generate a DEM from either...
air photo stereo imagery
(or the SPOT PAN overlap)
(or map contours)
- 2) Use the DEM to perform a BRCT
using a Lambertian model,
and the SPOT Panchromatic band.
- 3) Apply a spectral merge
between the TM imagery and
the corrected Panchromatic scene
(using the PCA substitution method)
- 4) Supervised classifications would then be derived from
 - the original TM data
 - the band ratio images
 - the spectral merge with BRCT-correction
- 5) Using ground-truth data from air-photo interpretations
 - evaluate the classification accuracy
 - determine success of various approaches

(Discuss, especially in the light of the land cover and topographic characteristics of the Cauca region)

The ultimate test of all this, ie which is the "Best" can only come from an evaluation of the usefulness of the end product. In other words, how well the product allows the questions of the Land Management group to be answered, by providing land cover data at the most appropriate compromise of spatial scale and thematic accuracy. Expert judgement will be needed in order to tell us this.

NOTES

Note | only a Lambertian model - may try Minnaert Constant to improve on this

Note | the correction does not identify topographic shadows - needs viewshed

Note | the problem of TM sensor striping - should have used a de-striping method first such as Crippen (1989).

Note | need for a 'quality' DEM to derive accurate slopes

1:25000 contours interpolated to 10m is just not good enough

REFERENCES

Dawes W, Hatton TJ (1993) TOPOG_IRM User Guide CSIRO Division of Water Resources, Australia.

Carper WJ, Lillesand TM, Kiefer RW (1990). The use of intensity-hue-saturation transformations for merging SPOT panchromatic and multispectral image data. *Photogrammetric Engineering and Remote Sensing* 56(4), 459-467.

Chavez PS, Sides, SC, Anderson JA (1991). Comparison of three different methods to merge multiresolution and multispectral data: Landsat TM and SPOT panchromatic. *Photogrammetric Engineering and Remote Sensing* 57(3), 295-303.

Cibula WG, Nyquist MO (1987). Use of topographic and climatological models in a geographical data base to improve Landsat MSS classification for Olympic National Park. *Photogrammetric Engineering and Remote Sensing* 53(1), 67-75.

Civco DL (1989). Topographic normalization of Landsat Thematic Mapper digital imagery. *Photogrammetric Engineering and Remote Sensing* 55(9), 1303-1309.

Cliche G, Bonn F, Teillet P (1985). Integration of the SPOT panchromatic channel into its multispectral mode for image sharpness enhancement. *Photogrammetric Engineering and Remote Sensing* 51(3), 311-316.

Colby JD (1991). Topographic normalization in rugged terrain. *Photogrammetric Engineering and Remote Sensing* 57(5), 531-537.

Conese C, Gilbert MA, Maselli F, Bottai, L (1993). Topographic normalization of TM scenes through the use of an atmospheric correction method and digital terrain models. *Photogrammetric Engineering and Remote Sensing* 59(12), 1745-1753.

Conese C, Maracchi G, Maselli F (1993). Improvement in maximum likelihood classification performance on highly rugged terrain using principal component analysis. *I.J.R.S.* ?

Crippen RE (1989). A simple spatial filtering routine for the cosmetic removal of scan-line noise from Landsat TM P-Tape imagery. *Photogrammetric Engineering and Remote Sensing* 55:3, 327-331.

Frank TD (1988). Mapping dominant vegetation communities in the Colorado Rock Mountain Front Range with Landsat Thematic Mapper and digital terrain data. *Photogrammetric Engineering and Remote Sensing* 54(12), 1727-1734.

Franklin SE, Wilson BA (1992). A three-stage classifier for remote sensing of mountain environments. *Photogrammetric Engineering and Remote Sensing* 58(4), 449-454.

Gilbert MA, Conese C, Maselli F (1992). An atmospheric correction method for the automatic retrieval of surface reflectances from TM images. Internal Report submitted to IJRS

Gratton DJ, Howarth PJ, Marceau DJ Combining DEM parameters with Landsat MSS and TM imagery in a GIS for mountain glacier characterisation. *IEEE Transactions on Geoscience and Remote Sensing* 28(4), 766-769.

Harris JR, Murray R, Hirose T (1990). IHS transform for the integration of radar imagery with other remotely sensed data. *Photogrammetric Engineering and Remote Sensing* 56(12), 1631-1641.

Hoben BN, Justice CO (1981). An examination of the spectral band ratio to reduce the topographic effect of remote sensing data. *I.J.R.S.* 2, 115-123.

Hutchinson MF (1988). A new procedure for gridding elevation and stream line data with automatic removal of pits. *J. Hydrol.* 106, 211-232.

Janssen L, Jaarsma N, van der Linden, E (1990). Integrating topographic data with remote sensing for land cover classification. *Photogrammetric Engineering and Remote Sensing* 56(11), 1503-1506.

Justice CO, Wharton SW, Holben BN (1981). Application of digital terrain data to quantify and reduce topographic effect on Landsat data. *Int. J. Remote Sensing* 2, 213-221.

Moody A, Woodcock CE (1994). Scale-dependent errors in the estimation of land-cover proportions: Implications for global land-cover datasets. *Photogrammetric Engineering and Remote Sensing* 60(5), 585-594.

Naugle BI, Lashlee JD (1992). Alleviating topographic influences on land cover classifications for mobility and combat modelling. *Photogrammetric Engineering and Remote Sensing* 58(8), 1217-1221.

Proy C, Tanr D, Deschamps PY (1989). Evaluation of topographic effects in remotely sensed data. *Remote Sensing of Environment* 30, 21-32.

Shettigara VK (1992). A generalized component substitution technique for spatial enhancement of multispectral images using a higher resolution data set. *Photogrammetric Engineering and Remote Sensing* 58(5), 561-567.

Walsh SJ, Bian L, Brown DG, Butler DR, Malanson GP (1989). Image enhancement of Landsat Thematic Mapper digital data for terrain evaluation, Glacier National Park, Montana, USA. *Geocarto International* 3, 55-58.

Welch R, Ehlers W (1987). Merging multiresolution SPOT HRV and Landsat TM data. *Photogrammetric Engineering and Remote Sensing* 53(3), 301-303.

Data Processing Operations

- The first task was to extract a subset of the full-scene images. Although the region to be rectified can be specified during the rectification process it is still quicker to display and move around a smaller sub-scene whilst collecting the GCP information.

A suitable sub-scene was identified using the Inquire Cursor feature whilst viewing the full-scene and identifying the file coordinates of a rectangular region that will encompass the area of interest.

The region selected must have reasonably generous margins around the actual study area to allow for the geometric rotation to be accommodated without losing data near to the study area margins. Keep a record of the coordinates of the subset.

- Before rectification via Ground Control Points two things needed to be done.
 - 1) any existing map projection information from the subscene image was removed (i.e. 'deleted') using *Image Info*
 - 2) the image was edge sharpened to assist in searching for and placing GCPs. This can be done using a high-pass convolution filter, or alternatively with the "crisp" process available in IMAGINE.

If using a convolution filter specify your own coefficients, as the defaults tend to be a bit harsh. Good results are normally achieved from

-1	-1	-1			-1	-1	-1
-1	14	-1	or		-1	16	-1
-1	-1	-1			-1	-1	-1

A sharpened image is only needed temporarily whilst locating GCPs - so only the 3 bands that are going to be used within the viewer (say 4,5,3 for a TM image) need to be processed and stored.

- The ground control points are located and entered using the GCP editor.

Ideally some 40 or so GCPs should be used for a top quality transformation, but in practice around 15 GCPs scattered evenly across the area of interest are usually sufficient. You can afford to drop some of these to get the reported RMS error down to an acceptable level, but the number should not drop below 8.

An RMS error of 0.5 pixels is usually taken as a good level of accuracy, although this obviously depends somewhat on the specific project requirements. It is relatively pointless struggling for very high spatial precision if the data are to be merged or processed with other information at lower levels of accuracy. For example, if the TM data is rectified to an RMS accuracy of 0.5 (i.e. 15m), the SPOT Pan image need only achieve an RMS of 1.5 (i.e. 15m) to be comparable. High spatial precision is desirable, but in practice the trade off between achieving a perfect rectification and getting the work done should be kept in balance.

Take an ASCII copy of the GCP matrix once it has been set up; it is very time consuming if you have to start again for any reason. To do this, select the 5 columns of interest, then press the R.H. mouse button while positioned over the POINTS heading. Select EXPORT and supply a suitable file name.

Once the RMS error is at an acceptable level and the transformation coefficients established, a rectification report can be generated in a similar manner.

- Compute the transformation equation to perform the projection to a Transverse Mercator. Again, it is wise to save a copy of the transformation coefficients to an ASCII file.

A 1st order transformation is acceptable for high resolution, narrow swath satellite imagery. 2nd order transformations or higher should be avoided. Although they may provide a better fit to the GCPs, the warping involved in achieving this can actually cause a higher degree of spatial inaccuracy overall.

- Perform the rectification.

The spatial resolution of all the tiles was specified as a 10m grid. Thus the TM and XS imagery is over-sampled. Cubic convolution interpolation was employed. This does alter radiometric values, and also led to complications with mosaicing (see later). However, the geometric integrity of the cubic convolution was believed to be important if cross-sensor spectral merging were to be performed later.

The final Cauca tiles are 5000x5000 pixels; the Cabuyal tiles are 2000x1500

- SPOT rectification

Two SPOT scenes are needed to cover the Cauca Study Area. Each image was rectified to the same Transverse Mercator projection separately, and then a mosaic or stitching operation was used to join these two sections together.

Since the images were acquired consecutively on a common orbital pass there was no need to use any form of histogram matching operation. However, for some reason (probably a bug) the mosaic program tends to transform the image data via its respective LUT while stitching. This means that the LUT of each section of image needs to be removed, or set to have no effect, before the images are stitched.

- SPOT mosaic operation

Although straightforward in principle, a complication arose due to the use of cubic convolution in the rectification stage. Basically, as the interpolation 'window' approaches and passes over the boundary of the unrectified image data the background zeros become incorporated into the interpolated output. This leads to a 'ramp' of decreasing values at the margins of the raw data files. When stitching two images, ERDAS will recognize a zero as the edge of the data. However, these non-zero values are not recognised and so become incorporated into the output as an unwanted artifact.

The solution found to this was rather messy. For the panchromatic bands the raster

editor can be used to manually remove the effected edge pixels and replace them with zero values. This is moderately time consuming but quite effective. Unfortunately, for the XS data the process proved to be even more arduous. The problem here is that the raster editor only edits the red band image (for a reason not understood). Thus the solution became more complex...

- subset a single band from the XS image
- use the raster editor to set the affected edge values to zero
- use reclass on this layer to code all non-zeros to 1
- multiply the full XS data by resulting mask
- but this generates a float type data file
- thus, rescale or truncate the results back to an 8-bit scale.

This worked, but it was pretty time consuming.
Maybe there's a better way?

- Generating the ratio bands.

In theory the OPERATORS function under Image Interpreter could be used to generate the ratio band images. In practice it was found to be easier to use the SPATIAL MODELLER, first of all defining the graphical model shown below. This was then used to generate a script model (again shown below) which is easily edited to generate any band ratio combination. This model selects the relevant bands from the multispectral image, applies a subtraction based atmospheric correction, performs the division operation (catching divide by zero), and finally rescales the result back onto an 8-bit range.

Corrections:

Atmospheric corrections are usually recommended before performing a ratio operation. The histogram subtraction method is the simplest to apply, although the regression model approach should be easy enough to implement using the large reservoir or cloud shadows to calibrate the coefficients (see the Imagine manual for further details of these methods). In the current study the subtraction method was adopted.

From a study of the spectral values found within cloud shadows (for bands 1&2) and the reservoir (for bands 3, 4, 5 & 7) the following correction factors were established (based on the integer average of 12 points)

- 1: subtract 46
- 2: subtract 14
- 3: subtract 11
- 4: subtract 5
- 5: subtract 2
- 7: subtract 1

Stacking:

Once the individual band ratios had been computed a graphical model was used to combine the layers into a single multi-band file. The model and its associated script are given below.

- Computing the Principal Components

There is a function in the Image Interpreter to perform this, but a graphical model was used

instead. PCA was performed on only 6 TM bands, the thermal band being excluded due to its discordant spatial resolution.

The Imagine Modelling Script was needed to derive an output of the Eigenvectors, Eigenvalues, and a correlation matrix. In fact, only a covariance matrix is computed by Imagine so a FORTRAN program was written to convert this into a correlation matrix. A FORTRAN program was also used to tidy up the output generated by Imagine.

APPENDIX I

Remotely sensed imagery acquired for the Cauca region

Landsat MSS imagery:

Date 24-Dec-87
Date 01-Feb-76

Landsat TM imagery:

Path/Row 9/58
Date 07-Aug-89

SPOT XS imagery:

2 images
Date 29-Aug-87

SPOT PAN imagery:

2 images
Date 29-Aug-87
Azi: 71.7
Elv: 67.1

SPOT Stereo Pair:

ordered for Aug/1994...

Air Photography:

Dates: 1989 (43...)
1991 (148...)
Scale: 1:36000
Scanning Resolution: 20X10-6
Panchromatic film

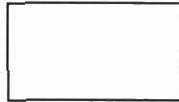
APPENDIX II

The dimensions of the study are were identified as indicated below:

Cauca Study Site Limits:

Latitude/Longitude

(76°45'W , 2°60'N)



(76°15'W , 2°35'N)

Transverse Mercator

(1035⁰⁰⁰ , 825⁰⁰⁰)



(1085⁰⁰⁰ , 775⁰⁰⁰)

Centre Scene: (1060⁰⁰⁰ , 800⁰⁰⁰)

Cabuyal Subset Limits:

(1052⁰⁰⁰ , 809⁰⁰⁰)



(1067⁰⁰⁰ , 789⁰⁰⁰)

Centre Scene: (1059⁵⁰⁰ , 799⁰⁰⁰)

"Bogota" Transverse Mercator Projection Details

Projection:	TM
Central Meridian	-77.082(02778)
Central Latitude	4.599(04722)
False Northing	1,000,000
False Easting	1,000,000
Scale along meridian	1.0

APPENDIX III

File structure and details of the imagery database

DIRECTORIES

The processed imagery for the Cauca Study Area have been stored under two principle directories, **/image2** and **/image** with a file naming convention as follows:

- 1) Unrectified subsets taken from the full-scene data, and rectified 50x50km Cauca tiles, are stored under the directory **/image2/mitch/**.

Rectified 15x20km Cabuyal tiles, which are subsets of the Cauca tiles, are stored under the **/image/cabuyal/** subdirectory, along with all subsequent data derived from processing and analysis.

- 2) Data obtained from different sensors are stored in separate subdirectories. All subdirectory names begin with either the letter **c**, to donate the Cauca study area, or the letter **s**, to donate the Cabuyal subset.

A subdirectory whose second letter is **u** indicates unrectified imagery, whilst **r** indicates rectified imagery.

The last 2 letters indicate the sensor from which the imagery are derived:

pn SPOT, panchromatic mode imagery
tm Landsat, Thematic Mapper imagery
xs SPOT, multispectral mode imagery

Thus, **/image2/mitch/cupn/** indicates Cauca data, unrectified, SPOT panchromatic images.
|and, **/image/cabuyal/crtm/** indicates Cabuyal data, rectified, Landsat TM images.

FILE NAMES

These are constructed as follows:

- 1) The first 4 characters replicate the information outlined above. I.e., **crtm**, **cuxs**, **srpn**, etc.
- 2) In the case of the SPOT imagery, this is then followed by either **N** or **S** to identify whether the imagery is obtained from the northern or southern full-scene SPOT image respectively, or by **NS** to indicate the stitched imagery.
- 3) The remaining characters specify the date of image acquisition:

Thus, **cutm07au89.img** = Cauca, unrectified, tm, 7th August 1989.
srpnNS29au87.img = Cabuyal, rectified, stitched, SPOT Pan., 29th August 1987.

4) Conventions for file endings is largely determined by ERDAS Imagine

- .img image file
- .cff Transformation coefficients file
- .gcc Rectification ground control points (GCPs)

However, the following will also be found...

- .rep A rectification report file
- .dat The GCP table (stored as an ASCII backup)
- .crp The transformation coefficients (stored as an ASCII backup)

Cauca Study Area Tiles

image2/mitch/crpn:

crpnN29au87.img	<i>Cauca tile, northern Pan. image</i>
crpnS29au87.img	<i>Cauca tile, southern Pan. image</i>
crpnNS29au87.img	<i>Cauca tile, stitched Pan. image</i>

image2/mitch/crtm:

crtm07au89.img	<i>Cauca tile, TM image</i>
----------------	-----------------------------

image2/mitch/crxs:

crxsN29au87.img	<i>Cauca tile, northern XS image</i>
crxsS29au87.img	<i>Cauca tile, southern XS image</i>
crxsNS29au87.img	<i>Cauca tile, stitched XS image</i>

image2/mitch/cupn:

* = N or S to indicate northern and southern scenes respectively

cupn*29au87.img	<i>Subset of SPOT Pan. image</i>
cupn*29au87.gcc	<i>Rectification GCPs</i>
cupn*29au87.dat	<i>GCP table (ASCII backup)</i>
cupn*29au87.cff	<i>Transformation Coefficients File</i>
cupn*29au87.crp	<i>Transformation Coefficients (ASCII backup)</i>
cupn*29au87.rep	<i>Rectification report</i>

/image2/mitch/cutm:

cutm07au89.img	<i>Subset of Landsat TM image</i>
cutm07au89.gcc	<i>Rectification GCPs</i>
cutm07au89.dat	<i>GCP table (ASCII backup)</i>
cutm07au89.cff	<i>Transformation Coefficients File</i>
cutm07au89.crp	<i>Transformation Coefficients (ASCII backup)</i>
cutm07au89.rep	<i>Rectification report</i>

image2/mitch/cuxs:

* = N or S to indicate northern and southern scenes respectively

cuxs*29au87.img	<i>Subset of SPOT XS image</i>
cuxs*29au87.gcc	<i>Rectification GCPs</i>
cuxs*29au87.dat	<i>GCP table (ASCII backup)</i>
cuxs*29au87.cff	<i>Transformation Coefficients File</i>
cuxs*29au87.crp	<i>Transformation Coefficients (ASCII backup)</i>
cuxs*29au87.rep	<i>Rectification report</i>

Cabuyal Study Area file structure

Directories:

image/

cabuyal/

srpn/ Cabuyal, rectified, Pan. imagery

srtm/ Cabuyal, rectified, TM imagery

srxs/ Cabuyal, rectified, XS imagery

ap-samples/ Segments of 42.IMG resampled

dem/ DTM data and derivatives

mixed/ TM-SPOT merged data files

classified/ Classified imagery

crocabu/ Vector outline of catchment

rios/ Vector rivers coverage

vias/ Vector roads coverage

crocabu.evs Vector properties

rios.evs "

vias.evs "

Files:

image/cabuyal/srpn/

srpnNS29au87.img Cabuyal tile, SPOT panchromatic image

image/cabuyal/srtm/

srtm07au89.img Cabuyal tile, Landsat TM image

srtm-pca.img Cabuyal tile, TM PCA bands

srtm6band.img Cabuyal tile, TM bands 1-5 & 7

tasseled.img Cabuyal tile, Tasseled Cap I-IV

image/cabuyal/srxs/

srxsNS29au87.img Cabuyal tile, SPOT XS image

image/cabuyal/ap-samples/

gt1EE.img Northern, most eastern air photo sample

gt1E.img Northern, eastern air photo sample

gt1W.img Northern, western air photo sample

gt1WW.img Northern, most western air photo sample

gt2EE.img Next south, most eastern air photo sample

etc..

/image/cabuyal/classified/mixed/

stmpn-ap.img 1st attempt at supervised classification

ap-fins.sig

ap-sigs.sig

stmpn.img

stmpn.sig

/image/cabuyal/classified/tm/super/

tm-ratios.img *Supervised, TM ratios*
tm-ratio-super.sig *Spectral sigs*

/image/cabuyal/classified/tm/unsupr/

error.img *"Error" image for level1.img*
level1.img *Unsupervised, TM ratios*
level1.sig *Spectral sigs. from ISODATA*
tm-bands.img *Unsupervised, Raw TM, 8 classes*
tm-bands.sig *Spectral sigs. from ISODATA*

/image/cabuyal/dem/

cabuyal-dem.img *DEM @10m from 1:25000, & Hutchinson*
mask.aoi *Raster of Cabuyal catchment as an area of interest*

brct-dem.img *DEM sample*
brct-asp.img *Computed slopes from DEM sample*
brct-slp.img *Computed aspects from DEM sample*
brct-img.img *SPOT Pan. sample*
brct-msk.img *Defines area of interest*
brct-out.img *BRCT corrected SPOT Pan.*

view*.img *3D views of Cabuyal, with TM/SPOT overlay*
view*.prm *Parameters of 3D view geometry*

image/cabuyal/mixed/

stmpn.img *Spectral merge of TM and Pan. (no correction)*
stmxspn.img *Spectral merge of TM/Pan./XS (no correction)*

/image/cabuyal/srtm/ratio/

rat-class.img
ratios-old.img *TM ratios - no correction*
ratios.img *TM ratios - with correction*
ratios.sig

Other files:

Map compositions are stored under

/users/mla/compose/

Graphical models are stored under

/users/mla/gmodels/

The directories and file names should be self-explanatory.

APPENDIX IV

LANDSAT TM PRE-PROCESSING DETAILS

Sub-scene coordinates from full-scene image:

ULX	1750	LRX	4050
ULY	2400	LRY	4500

GCP Table:

1	GCP #1	755.82	827.65	1049660	809310
2	GCP #2	587.35	686.00	1045500	814000
3	GCP #3	700.39	812.07	1048150	810000
4	GCP #4	910.36	827.88	1054050	808710
5	GCP #5	1074.06	872.81	1058460	806750
6	GCP #6	991.06	969.81	1055730	804380
7	GCP #7	708.88	1059.62	1047460	803020
8	GCP #8	1057.62	731.62	1058550	810840
9	GCP #9	1217.62	809.12	1062780	807990
10	GCP #10	1356.81	1165.94	1065250	797370
11	GCP #11	1368.81	1359.56	1064750	791800
12	GCP #12	723.03	1437.84	1046260	792250

Transformation Coefficients:

1st order Transformation of cutm07au89.img

Imagine Tabular Report

Row	X'	Y'
1	-31629.312606	34160.599451
2	0.034716	-0.004961
3	-0.005010	-0.034752

Rectification Report:

RMS error report
cutm07au89.img

Reported Total RMS error: **0.463281**

Imagine Tabular Report

Row	Point ID	X Residual	Y Residual	RMS Error	Contribution
1	GCP #1	-0.119	0.527	0.541	1.167
2	GCP #2	0.434	-0.174	0.468	1.009
3	GCP #3	-0.567	-0.381	0.684	1.475
5	GCP #5	-0.032	0.679	0.680	1.467
6	GCP #6	0.068	-0.416	0.421	0.909
9	GCP #9	0.168	-0.154	0.228	0.492
10	GCP #10	-0.064	-0.158	0.170	0.368
12	GCP #12	0.113	0.077	0.137	0.296
13	GCP #13	0.000	0.000	0.000	0.000
Count	9	9	9	9	9
Mean	N/A	/	-0.000	0.370	0.798
Minimum	N/A	/	-0.567	0.000	0.000
Maximum	N/A	/	0.434	0.684	1.475
Stddev	N/A	/	0.268	0.378	0.532

Erdas Imagine File Information

File Name : crtm08au89.img
Last Modified : Sat Aug 6 12:12:17 1994
Number of Layers : 7

Layer Information:

Name : :Layer_1
Width : 5001
Height : 5001
Type : Continuous
Block Width : 64
Block Height : 64
Pixel Depth : Unsigned 8-bit
Compression Type : None

Statistics :

Last Modified : Sat Aug 6 12:12:17 1994
Maximum Value : 255.000000
Minimum Value : 25.000000
Mean : 63.944597
Median : 57.000000
Mode : 56.000000
Standard Deviation : 32.713322

Projection Information :

Projection Zone : 0
Spheroid Name : WGS 84
Georeferenced to : Transverse Mercator

Map Information :

Upper Left center X : 1035000.000000
Upper Left center Y : 825000.000000
Lower Right center X: 1085000.000000
Lower Right center Y: 775000.000000
Pixel X size : 10.000000
Pixel Y size : 10.000000

SPOT XS PRE-PROCESSING DETAILS

Northern Image

Sub-scene coordinates from full-scene image:

ULX	0	LRX	3195
ULY	1700	LRY	3002

GCP Table:

1	GCP #1	434.77	562.38	1046640	812280
2	GCP #2	607.05	590.96	1049940	811220
3	GCP #3	784.07	611.76	1053330	810260
4	GCP #4	1271.82	798.83	1062500	805060
5	GCP #5	1460.12	888.90	1065880	802730
6	GCP #6	1389.62	1104.50	1068700	798830
7	GCP #7	1560.67	1088.86	1067240	798500
8	GCP #8	1454.79	1231.64	1064710	795950
9	GCP #9	1054.68	1200.63	1056940	797840
10	GCP #10	824.87	1217.95	1052740	798130
11	GCP #11	488.67	1099.78	1046020	801490
12	GCP #12	461.63	757.45	1046070	819480

Transformation Coefficients:

1st order Transformation of cuxsN29au87.img

Imagine Tabular Report

Row	X'	Y'
1	-4467.476696	48465.167462
2	0.049414	-0.007504
3	-0.007775	-0.049304

Rectification Report:

RMS error report
cuxsN29au87.img

Reported Total RMS error: **0.7672**

Imagine Tabular Report

Row	Point ID	X Residual	Y Residual	RMS Error	Contribution
1	GCP #1	0.499	0.542	0.736	0.960
2	GCP #2	-0.475	-0.538	0.718	0.93
5	GCP #5	0.117	0.501	0.515	0.671
7	GCP #7	-0.342	-1.109	1.160	1.512
8	GCP #8	0.348	0.821	0.891	1.162
11	GCP #11	-0.146	-0.217	0.262	0.341
Count	6	6	6	6	6
Mean	N/A	-0.000	-0.000	0.714	0.930
Minimum	N/A	-0.475	-1.109	0.262	0.341
Maximum	N/A	0.499	0.821	1.160	1.512
Stddev	N/A	0.387	0.746	0.308	0.402

Erdas Imagine File Information

File Name : crxsNS29au87.img
Last Modified : Mon Aug 29 16:01:27 1994
Number of Layers : 3

Layer Information:

Name : :Layer_1
Width : 5001
Height : 5001
Type : Continuous
Block Width : 64
Block Height : 64
Pixel Depth : Unsigned 8-bit
Compression Type : None

Statistics :

Last Modified : Mon Aug 29 16:01:27 1994
Maximum Value : 255.000000
Minimum Value : 0.000000
Mean : 49.090765
Median : 44.000000
Mode : 0.000000
Standard Deviation : 37.807094

Projection Information :

Projection Zone : 0
Spheroid Name : WGS 84
Georeferenced to : Transverse Mercator

Map Information :

Upper Left center X : 1035020.000000
Upper Left center Y : 825000.000000
Lower Right center X: 1085020.000000
Lower Right center Y: 775000.000000
Pixel X size : 10.000000
Pixel Y size : 10.000000

Southern Image

Full-scene image was processed:

GCP Table:

1	West Side Inter	839.312	935.812	1046123.44	781922.81
2	Mid Intersect	1316.187	862.187	1055771.56	781932.19
3	N-Mid Intersect	1310.210	526.300	1056685.31	788596.56
4	W Side Main Rd	1474.656	707.406	1059371.25	784526.25
5	W of Main Rd	1322.531	129.531	1058136.25	796393.75
6	S of main Rd	1500.350	567.076	1060317.81	787243.44
7	North of Fork	1609.031	955.531	1061280.62	779230.62
8	South of Bend	449.781	328.343	1040316.25	795081.25
9	NW Intersect	909.281	193.281	1049793.44	796387.19
10	tie #10	381.437	116.812	1039548.75	799456.25
11	tie #11	835.812	58.812	1048703.75	799236.25
12	tie #12	1468.062	162.812	1060876.25	795276.25
13	tie #13	2611.156	66.968	1083768.12	793733.12

Transformation Coefficients:

1st order Transformation of cuxsS29au87.img

Imagine Tabular Report

Row	X'	Y'
1	-44973.377384	47565.946814
2	0.049446	-0.007538
3	-0.007563	-0.049550

Rectification Report:

RMS error report
cuxsS29au87.img

Reported Total RMS error: **0.455788**

Imagine Tabular Report

Row	Point ID	X Residual	Y Residual	RMS Error	Contribution
1	1 West Side Inter	-0.148	0.214	0.260	0.571
2	2 Mid Intersect	-0.037	0.648	0.649	1.425
3	3 N-Mid Intersect	0.718	-0.572	0.918	2.015
4	4 W Side Main Rd	-0.136	-0.241	0.276	0.606
7	7 North of Fork	-0.051	-0.359	0.363	0.796
10	tie #10	0.034	-0.011	0.036	0.079
11	tie #11	-0.003	-0.119	0.119	0.261
12	tie #12	-0.428	0.345	0.550	1.206
13	tie #13	0.050	0.095	0.107	0.235
Count	9	9	9	9	9
Mean	N/A	0.000	-0.000	0.364	0.799
Minimum	N/A	-0.428	-0.572	0.036	0.079
Maximum	N/A	0.718	0.648	0.918	2.015
Stddev	N/A	0.306	0.375	0.291	0.637

SPOT PAN. PRE-PROCESSING DETAILS

Northern Image

Sub-scene coordinates from full-scene image:

ULX	0	LRX	6380
ULY	3000	LRY	6005

GCP Table:

1	GCP #1	763.37	1547.62	1046640	812280
2	GCP #2	1107.87	1606.12	1049940	811220
3	GCP #3	1461.12	1647.62	1053330	810260
4	GCP #4	1605.12	1813.12	1054575	808400
5	GCP #5	1777.38	1762.38	1056270	808620
6	GCP #6	2034.12	1854.62	1058730	807325
7	GCP #7	2050.12	1669.62	1059150	809160
8	GCP #8	2439.38	2020.62	1062500	805060
9	GCP #9	2813.87	2199.62	1065880	802730
10	GCP #10	2635.62	1544.12	1065140	809470
11	GCP #11	3152.51	2543.64	1068670	798850
12	GCP #12	2561.87	815.30	1065550	816850
13	GCP #13	2836.91	2947.78	1064920	795340
14	GCP #14	2367.13	2686.21	1060730	798600
15	GCP #15	338.41	2885.71	1040356	799705
16	GCP #16	1230.07	2781.14	1049329	799392
17	GCP #17	2004.09	2826.22	1056910	797792
18	GCP #18	3247.05	2745.20	1069330	796723

Transformation Coefficients:

1st order Transformation of cupn29au87.img

Imagine Tabular Report

Row	X'	Y'
1	-90071.823432	97426.571011
2	0.098816	-0.015012
3	-0.015497	-0.098690

Rectification Report:

RMS error report
cupnN29au87.img

Reported Total RMS error: **0.632958**

Imagine Tabular Report

Row	Point ID	X Residual	Y Residual	RMS Error	Contribution
2	GCP #2	-0.525	-0.778	0.938	1.482
7	GCP #7	-0.758	0.763	1.075	1.699
12	GCP #12	0.741	-0.002	0.741	1.171
13	GCP #13	-0.301	-0.366	0.474	0.748
14	GCP #14	0.211	0.160	0.265	0.418
15	GCP #15	0.337	-0.073	0.345	0.545
16	GCP #16	0.200	0.680	0.709	1.120
17	GCP #17	0.088	-0.300	0.312	0.494
18	GCP #18	0.006	-0.084	0.084	0.133
Count	9	9	9	9	9
Mean	N/A	0.000	0.000	0.549	0.868
Minimum	N/A	-0.758	-0.778	0.084	0.133
Maximum	N/A	0.741	0.763	1.075	1.699
Stddev	N/A	0.460	0.489	0.334	0.527

Erdas Imagine File Information

File Name : crpnNS29au87.img
Last Modified : Fri Aug 26 18:44:51 1994
Number of Layers : 1

Layer Information:

Name : :Layer_1
Width : 5001
Height : 5000
Type : Continuous
Block Width : 64
Block Height : 64
Pixel Depth : Unsigned 8-bit
Compression Type : None

Statistics :

Last Modified : Fri Aug 26 18:44:51 1994
Maximum Value : 255.000000
Minimum Value : 0.000000
Mean : 43.798342
Median : 42.000000
Mode : 0.000000
Standard Deviation : 38.235842

Projection Information :

Projection Zone : 0
Spheroid Name : WGS 84
Georeferenced to : Transverse Mercator

Map Information :

Upper Left center X : 1035000.000000
Upper Left center Y : 825000.000000
Lower Right center X: 1085000.000000
Lower Right center Y: 775010.000000
Pixel X size : 10.000000
Pixel Y size : 10.000000

APPENDIX V

The backup archive on exabyte tape contains:

block 1

rw-rw-r--x101/11 392059787 Aug 4 16:56 1994 cauca.img

block 2

rw-rw-r--133/26 1915 Aug 12 13:50 1994 cuxsN29au87.cff
rw-rw-r--133/26 385 Aug 16 08:54 1994 cuxsN29au87.crp
rw-rw-r--133/26 555 Aug 29 11:18 1994 cuxsN29au87.dat
rw-rw-r--133/26 7453 Aug 12 13:54 1994 cuxsN29au87.gcc
rw-rw-r--133/26 629900 Aug 17 16:23 1994 cuxsN29au87.img
rw-rw-r--133/26 1117 Aug 29 11:27 1994 cuxsN29au87.rep
rw-rw-r--133/26 3937 Aug 29 08:48 1994 cuxsS29au87.cff
rw-rw-r--133/26 305 Aug 29 09:26 1994 cuxsS29au87.crp
rw-rw-r--133/26 832 Aug 29 08:47 1994 cuxsS29au87.dat
rw-rw-r--133/26 4957 Aug 29 08:49 1994 cuxsS29au87.gcc
rw-rw-r--133/26 39204410 Aug 29 11:24 1994 cuxsS29au87.img
rw-rw-r--133/26 1445 Aug 29 09:13 1994 cuxsS29au87.rep

block 3

rw-rw-r--133/26 1915 Aug 29 09:14 1994 cutm07au89.cff
rw-rw-r--133/26 323 Aug 29 09:26 1994 cutm07au89.crp
rw-rw-r--133/26 587 Aug 29 08:58 1994 cutm07au89.dat
rw-rw-r--133/26 5821 Aug 5 18:36 1994 cutm07au89.gcc
rw-rw-r--133/26 46468238 Aug 26 09:13 1994 cutm07au89.img
rw-rw-r--133/26 1464 Aug 29 09:13 1994 cutm07au89.rep

block 4

rw-rw-r--133/26 4001 Aug 26 18:21 1994 cupnN29au87.cff
rw-rw-r--133/26 426 Aug 29 11:53 1994 cupnN29au87.crp
rw-rw-r--133/26 629 Aug 29 11:39 1994 cupnN29au87.dat
rw-rw-r--133/26 14023 Aug 26 18:08 1994 cupnN29au87.gcc
rw-rw-r--133/26 19335920 Aug 26 18:07 1994 cupnN29au87.img
rw-rw-r--133/26 1431 Aug 29 11:51 1994 cupnN29au87.rep

block 5

rw-rw-r--133/26 51639203 Aug 29 15:28 1994 crxs/crxsN29au87.img
rw-rw-r--133/26 128 Aug 29 08:04 1994 crxs/crxsNS.flr
rw-rw-r--133/26 76965023 Aug 29 16:10 1994 crxs/crxsNS29au87.img
rw-rw-r--133/26 910 Aug 29 16:13 1994 crxs/crxsNS29au87.info
rw-rw-r--133/26 38976293 Aug 29 13:06 1994 crxs/crxsS29au87.img

block 6

rw-rw-r--133/26 910 Aug 16 08:57 1994 crtm/crtm07au89.info
rw-rw-r--133/26 241142659 Aug 26 16:42 1994 crtm/crtm08au89.img

block 7

rw-rw-r--133/26 17872421 Aug 26 18:55 1994 crpn/crpnN29au87.img
rw-rw-r--133/26 120 Aug 26 18:43 1994 crpn/crpnNS.flr
rw-rw-r--133/26 34452766 Aug 27 11:12 1994 crpn/crpnNS29au87.img
rw-rw-r--133/26 910 Aug 27 11:13 1994 crpn/crpnNS29au87.info
rw-rw-r--133/26 14313403 Aug 27 10:59 1994 crpn/crpnS29au87.img

block 8

rw-rw-r--x133/26 0 Aug 16 09:03 1994 cabuyal/crocabu/
rw-rw-r--133/26 48 Aug 16 09:03 1994 cabuyal/crocabu/tic
rw-rw-r--133/26 16 Aug 16 09:03 1994 cabuyal/crocabu/bnd
rw-rw-r--133/26 96 Aug 16 09:03 1994 cabuyal/crocabu/tol
rw-rw-r--133/26 355 Aug 24 14:04 1994 cabuyal/crocabu/log
rw-rw-r--133/26 132 Aug 16 09:03 1994 cabuyal/crocabu/lab
rw-rw-r--133/26 144 Aug 16 09:03 1994 cabuyal/crocabu/cnt
rw-rw-r--133/26 116 Aug 16 09:03 1994 cabuyal/crocabu/cnx
rw-rw-r--133/26 96 Aug 16 09:03 1994 cabuyal/crocabu/pat
rw-rw-r--133/26 5708 Aug 16 09:03 1994 cabuyal/crocabu/arc
rw-rw-r--133/26 116 Aug 16 09:03 1994 cabuyal/crocabu/arc
rw-rw-r--133/26 216 Aug 16 09:03 1994 cabuyal/crocabu/pal
rw-rw-r--133/26 116 Aug 16 09:03 1994 cabuyal/crocabu/pax
rw-rw-r--133/26 9691 Aug 16 09:12 1994 cabuyal/crocabu.evs

rw-rw-r--x133/26 0 Aug 24 14:24 1994 cabuyal/info/
rw-rw-r--133/26 4180 Aug 24 14:24 1994 cabuyal/info/arcdr9
rw-rw-r--132/26 432 Aug 19 16:25 1994 cabuyal/info/arc000nit
rw-rw-r--132/26 80 Aug 19 16:25 1994 cabuyal/info/arc000dat
rw-rw-r--132/26 576 Aug 19 16:25 1994 cabuyal/info/arc001nit
rw-rw-r--132/26 80 Aug 19 16:25 1994 cabuyal/info/arc001dat
rw-rw-r--132/26 576 Aug 19 16:25 1994 cabuyal/info/arc002nit
rw-rw-r--132/26 80 Aug 19 16:25 1994 cabuyal/info/arc002dat

rw-rw-r--133/26	432	Aug 24 14:04 1994	cabuyal/info/arc003nit
rw-rw-r--133/26	432	Aug 24 14:04 1994	cabuyal/info/arc004nit
rw-rw-r--133/26	80	Aug 24 14:04 1994	cabuyal/info/arc003dat
rw-rw-r--133/26	80	Aug 24 14:04 1994	cabuyal/info/arc004dat
rw-rw-r--133/26	576	Aug 24 14:04 1994	cabuyal/info/arc005nit
rw-rw-r--133/26	576	Aug 24 14:04 1994	cabuyal/info/arc006nit
rw-rw-r--133/26	80	Aug 24 14:04 1994	cabuyal/info/arc005dat
rw-rw-r--133/26	80	Aug 24 14:04 1994	cabuyal/info/arc006dat
rw-rw-r--133/26	432	Aug 24 14:04 1994	cabuyal/info/arc007nit
rw-rw-r--133/26	80	Aug 24 14:04 1994	cabuyal/info/arc007dat
rw-rw-r--133/26	576	Aug 24 14:04 1994	cabuyal/info/arc008nit
rw-rw-r--133/26	80	Aug 24 14:04 1994	cabuyal/info/arc008dat
rw-rw-r--133/26	432	Aug 24 14:24 1994	cabuyal/info/arc009nit
rw-rw-r--133/26	80	Aug 24 14:24 1994	cabuyal/info/arc009dat
rw-rw-r--133/26	576	Aug 24 14:24 1994	cabuyal/info/arc010nit
rw-rw-r--133/26	80	Aug 24 14:24 1994	cabuyal/info/arc010dat
rw-rw-r--133/26	0	Aug 19 16:25 1994	cabuyal/jorge/
rw-rw-r--132/26	48	Aug 19 16:25 1994	cabuyal/jorge/tic
rw-rw-r--132/26	16	Aug 19 16:25 1994	cabuyal/jorge/bnd
rw-rw-r--132/26	292	Aug 19 16:25 1994	cabuyal/jorge/lab
rw-rw-r--132/26	120	Aug 19 16:25 1994	cabuyal/jorge/tol
rw-rw-r--132/26	321	Aug 19 16:25 1994	cabuyal/jorge/log
rw-rw-r--132/26	374	Aug 19 16:25 1994	cabuyal/jorge/prj
rw-rw-r--132/26	96	Aug 19 16:25 1994	cabuyal/jorge/pat
rw-rw-r--132/26	9840	Aug 19 16:34 1994	cabuyal/jorge.evs
rw-rw-r--132/26	205	Aug 24 14:30 1994	cabuyal/log
rw-rw-r--133/26	0	Aug 16 09:03 1994	cabuyal/rios/
rw-rw-r--133/26	48	Aug 16 09:03 1994	cabuyal/rios/tic
rw-rw-r--133/26	16	Aug 16 09:03 1994	cabuyal/rios/bnd
rw-rw-r--133/26	2023	Aug 24 14:04 1994	cabuyal/rios/log
rw-rw-r--133/26	96	Aug 16 09:03 1994	cabuyal/rios/tol
rw-rw-r--133/26	140	Aug 16 09:03 1994	cabuyal/rios/cnt
rw-rw-r--133/26	116	Aug 16 09:03 1994	cabuyal/rios/cnx
rw-rw-r--133/26	32	Aug 16 09:03 1994	cabuyal/rios/pat
rw-rw-r--133/26	116	Aug 16 09:03 1994	cabuyal/rios/pfx
rw-rw-r--133/26	326236	Aug 16 09:03 1994	cabuyal/rios/arc
rw-rw-r--133/26	100	Aug 16 09:03 1994	cabuyal/rios/lab
rw-rw-r--133/26	6996	Aug 16 09:03 1994	cabuyal/rios/arx
rw-rw-r--133/26	56892	Aug 16 09:03 1994	cabuyal/rios/aat
rw-rw-r--133/26	32868	Aug 16 09:03 1994	cabuyal/rios/msk
rw-rw-r--133/26	893	Aug 16 09:03 1994	cabuyal/rios/aeproprs.aml
rw-rw-r--133/26	15792	Aug 16 09:03 1994	cabuyal/rios/pff
rw-rw-r--133/26	9791	Aug 23 19:25 1994	cabuyal/rios.evs
rw-rw-r--133/26	0	Aug 27 11:05 1994	cabuyal/srpn/
rw-rw-r--133/26	3162617	Aug 27 11:06 1994	cabuyal/srpn/srpnNS29au87.img
rw-rw-r--133/26	0	Aug 25 11:58 1994	cabuyal/srtm/
rw-rw-r--133/26	29548886	Aug 29 16:32 1994	cabuyal/srtm/srtm08au89.img
rw-rw-r--133/26	0	Aug 24 19:21 1994	cabuyal/srtm/ratio/
rw-rw-r--133/26	18966116	Aug 29 16:45 1994	cabuyal/srtm/ratio/r54-53-43-75-74-32.img
rw-rw-r--133/26	612	Aug 12 15:03 1994	cabuyal/srtm/ratio/rat43.mdl
rw-rw-r--133/26	612	Aug 12 15:04 1994	cabuyal/srtm/ratio/rat53.mdl
rw-rw-r--133/26	612	Aug 12 15:06 1994	cabuyal/srtm/ratio/rat54.mdl
rw-rw-r--133/26	798	Aug 12 15:44 1994	cabuyal/srtm/ratio/ratstack.mdl
rw-rw-r--133/26	47	Aug 24 19:21 1994	cabuyal/srtm/ratio/hml.plt
rw-rw-r--133/26	334	Aug 24 19:21 1994	cabuyal/srtm/ratio/printers.hml.plt.cfg
rw-rw-r--133/26	1621086	Aug 24 19:21 1994	cabuyal/srtm/ratio/hml.plt.panel_0
rw-rw-r--133/26	84	Aug 24 19:21 1994	cabuyal/srtm/ratio/hml.plt.panel_0.name
rw-rw-r--133/26	12645640	Aug 29 16:43 1994	cabuyal/srtm/tasseled.img
rw-rw-r--133/26	0	Aug 24 08:54 1994	cabuyal/srtm/pca/
rw-rw-r--133/26	75597035	Aug 29 16:48 1994	cabuyal/srtm/pca/pca.img
rw-rw-r--133/26	3162617	Aug 22 08:05 1994	cabuyal/srtm/pca/pca1x.img
rw-rw-r--133/26	3162617	Aug 22 14:14 1994	cabuyal/srtm/pca/pca2x.img
rw-rw-r--133/26	3162617	Aug 22 14:15 1994	cabuyal/srtm/pca/pca3x.img
rw-rw-r--133/26	3162617	Aug 22 14:16 1994	cabuyal/srtm/pca/pca4x.img
rw-rw-r--133/26	3162617	Aug 22 14:17 1994	cabuyal/srtm/pca/pca5x.img
rw-rw-r--133/26	3162617	Aug 22 18:26 1994	cabuyal/srtm/tm5x.img
rw-rw-r--133/26	0	Aug 27 10:59 1994	cabuyal/srtm/unsuper/
rw-rw-r--133/26	3162617	Aug 19 07:44 1994	cabuyal/srtm/unsuper/rat-offset.img
rw-rw-r--133/26	4225685	Aug 29 16:53 1994	cabuyal/srtm/unsuper/rat-unclas.img
rw-rw-r--133/26	3168920	Aug 29 16:54 1994	cabuyal/srtm/unsuper/rat2-unclas.img
rw-rw-r--133/26	60912	Aug 24 09:42 1994	cabuyal/srtm/unsuper/rat2-unclas.sig
rw-rw-r--133/26	3183660	Aug 24 18:36 1994	cabuyal/srtm/unsuper/rat2-smth.img

rw-rw-r--133/26	3166404	Aug 29 16:51 1994	cabuyal/srtm/unsuper/rat-tass.img
rw-rw-r--133/26	3181145	Aug 24 18:47 1994	cabuyal/srtm/unsuper/hml.img
rw-rw-r--133/26	29766	Aug 25 09:34 1994	cabuyal/srtm/unsuper/rat-tass.sig
rw-rw-r--133/26	57293	Aug 12 16:16 1994	cabuyal/srtm/unsuper/rat-unclas.sig
rw-rw-r--133/26	3169187	Aug 19 10:08 1994	cabuyal/srtm/unsuper/rat-smth.img
rw-rw-r--133/26	3003501	Aug 17 11:50 1994	cabuyal/srtm/unsuper/rat.dat
rw-rw-r--133/26	1587833	Aug 19 11:11 1994	cabuyal/srtm/unsuper/rat-denx.img
rw-rw-r--133/26	1592655	Aug 19 10:59 1994	cabuyal/srtm/unsuper/rat-cplx.img
rw-rw-r--133/26	0	Aug 24 19:16 1994	cabuyal/srtm/unsuper/plots/
rw-rw-r--133/26	115402	Aug 24 19:16 1994	cabuyal/srtm/unsuper/plots/hml.map.ovr
rw-rw-r--133/26	821	Aug 24 19:16 1994	cabuyal/srtm/unsuper/plots/hml.map
rw-rw-r--133/26	0	Aug 29 16:41 1994	cabuyal/srxs/
rw-rw-r--133/26	9482933	Aug 29 16:11 1994	cabuyal/srxs/srxsNS29au87.img
rw-rw-r--133/26	0	Aug 24 14:24 1994	cabuyal/test/
rw-rw-r--133/26	48	Aug 24 14:24 1994	cabuyal/test/tic
rw-rw-r--133/26	16	Aug 24 14:24 1994	cabuyal/test/bnd
rw-rw-r--133/26	45	Aug 24 14:24 1994	cabuyal/test/log
rw-rw-r--133/26	0	Aug 16 09:03 1994	cabuyal/vias/
rw-rw-r--133/26	48	Aug 16 09:03 1994	cabuyal/vias/tic
rw-rw-r--133/26	16	Aug 16 09:03 1994	cabuyal/vias/bnd
rw-rw-r--133/26	96	Aug 16 09:03 1994	cabuyal/vias/tol
rw-rw-r--133/26	1444	Aug 24 14:30 1994	cabuyal/vias/log
rw-rw-r--133/26	100	Aug 16 09:03 1994	cabuyal/vias/lab
rw-rw-r--133/26	352	Aug 16 09:03 1994	cabuyal/vias/pat
rw-rw-r--133/26	16356	Aug 16 09:03 1994	cabuyal/vias/arc
rw-rw-r--133/26	932	Aug 16 09:03 1994	cabuyal/vias/arx
rw-rw-r--133/26	6240	Aug 16 09:03 1994	cabuyal/vias/aat
rw-rw-r--133/26	696	Aug 16 09:03 1994	cabuyal/vias/nrf
rw-rw-r--133/26	10705	Aug 24 15:59 1994	cabuyal/vias.evs